

# Design a Model with Dual Band Frequency Selective Surface (FSS) & Impedance Modeling Assumptions

Payal Jindal<sup>1</sup>, Dr. Sudheer Sharma<sup>2</sup>

<sup>1</sup> Research Scholar, Department of Electronics & Communication, Jaipur National University, Jaipur, Rajasthan, India.

<sup>2</sup> Department of Electronics & Communication, Jaipur National University, Jaipur, Rajasthan, India.

**Abstract** – This paper shows a specific design of an antenna with an enhanced gain bandwidth in the RF range. This design FSS structure consists of a square Frequency Selective Surface (FSS) structure placed on a substrate. In this paper, I am using FR4 substrate. The circular and square slot is added on the FSS sheet to modify this design. The enhancement of bandwidth of the antenna is attributed to the positive reflection phase gradient of an electromagnetic band gap (EBG) structure. The proposed FSS is a multilevel metallic hole array (MHA) working at 8 GHz. Results show an increment of the maximum gain of 8 dB with regard to a single open waveguide, with a small increment of the antenna's height.

**Index Terms** – Antenna, high gain, wide bandwidth, Effective shielding, Electromagnetic interference, FSS, Metamaterial, Periodic Structures, Ultra-wideband.

## 1. INTRODUCTION

To achieve an amount of spectral output for the FSS structure, lot of parameters or variables can be changed such as the dimensions of periodicity, slot size, shape, thickness of dielectric substrate and constant, and number of sweeps per second. Frequency selective surfaces (FSSs) have important military and civilian applications and many other applications in various fields including antenna theory, satellite communications and stealth technology. It is a very new technique to introduce new results for industry point of view.

The aim of the proposed antenna is to enhance the gain of an open rectangular waveguide but keeping its low-profile.

## 2. UNIT CELL: METALLIC HOLE

The unit cell of the metallic hole antenna is a perfect square sheet that is completely metallic. The center frequency of the metallic sheet is defined by width, sweep period. The shape and size of the unit cell is determined by the bandwidth of the hole [6]. The shape of holes possibly are square, with a width  $w=0.7$ , in order to increase the bandwidth and we can change the angle of any variation parameter without changing the amplitude of the input signal.

Nowadays FSS have very wide applications to increase the radiation of an antenna. For example, a frequency selective surface based on substrate integrated technology [5], is placed on the aperture of a horn to form the so-called *antenna*. Resulting

structure is likely to reflect interference signals at the frequencies located out of the transmission band of the FSS.

## 3. FSS DESIGN

The geometry of the unit cell of this design is made up of square and circular cutouts hatched on the dielectric substrate. The unit cell of this double slot FSS design is also shown in the figure. The double slot FSS is designed made up of copper with a thickness of 0.035 mm. In this paper, the FSS is hatched on the FR4 substrate (210 mm × 210 mm) for 7 × 7 elements. The two materials of dielectric substrate used in this paper are FR4 board and glass. The dielectric constant of FR4 is 4.4 and a tangent loss of 0.019 with a thickness of 1.6 mm, while the glass dielectric constant is 6.9 and conductivity is S/m with a thickness of 5 mm. The double slot FSS is designed and simulated in this paper.

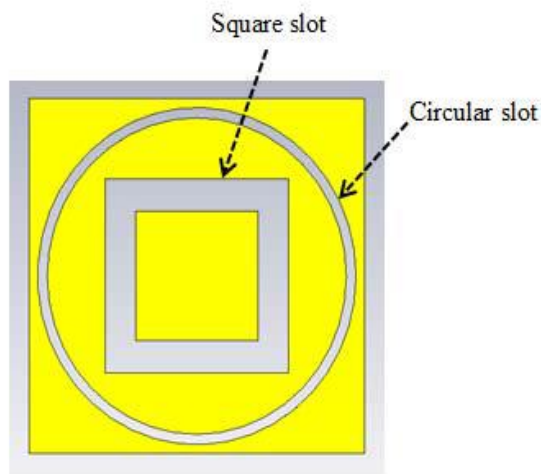


Fig. 1. Geometry of the design FSS structure

The main characteristics of the antenna, such as its operating frequency, directivity, gain and width and radiation patterns are determined by the property of the PRS. The operating frequency depends on the following equation [7],

$$f = \frac{c}{4\pi h} (\varphi_H + \varphi_L - 2N\pi), \quad N = 0, 1, 2, \dots$$

#### 4. FSS HYBRID MATERIAL

There are six types of configurations investigated in this paper based on two metas. The dielectric constant tangent loss of 0.019 with a thickness of glass dielectric constant is 6.9 and conduction S/m with thickness of 5 mm. The double sketched on the FR4 board. Then the glass is of the FR4 board and on the double slot FSS is paper because of  $\epsilon_s$  at -0.5 dB at 2.4 to others designed. cy response needed 4 GHz frequency circular slot. The slot FSS structure cube slot FSS ( $7 \times 7$ ) FSS prototype ons that will be trials (FR4+glass) of FR4 is 4.4 and a 1.6 mm while the structure is placed at the back S structure. The inclusion of additional layers increments the maximum phase shift that can be reached by a single layer. Fig. 2a shows the 3-layer unit cell considered in this paper. All layers have the same dimensions ( $p$  and  $w$ ) and are apart a distance  $s$ . Fig.2b shows the transmission parameter of the unit cell computed with Analysis with the help of HFSS [7] at 8 GHz for several periods ( $w=0.9p$ ). In these simulations, periodic boundary conditions have been applied to the four lateral walls and Fouquet ports.

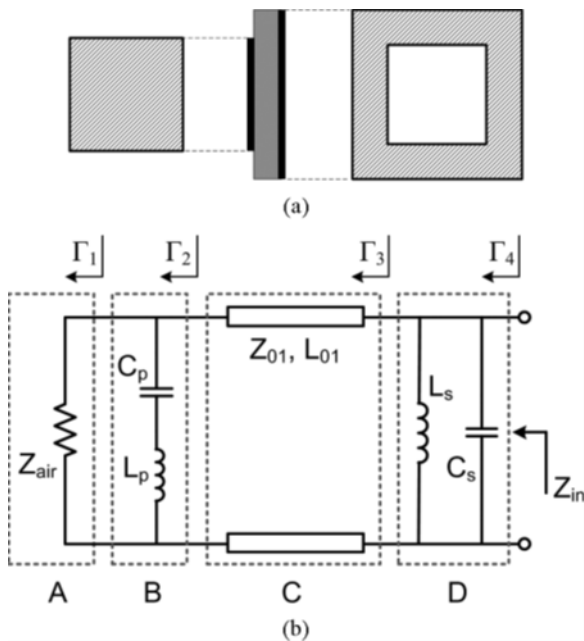
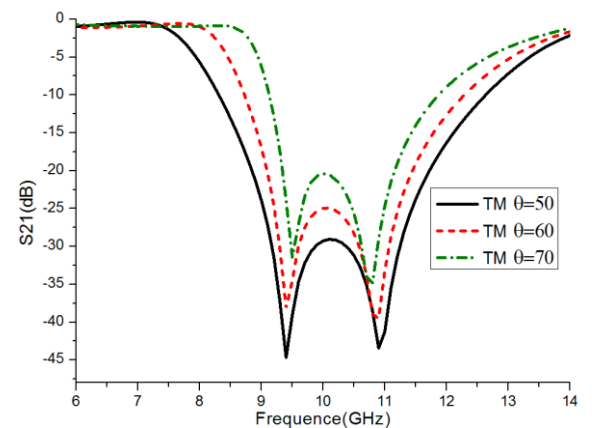
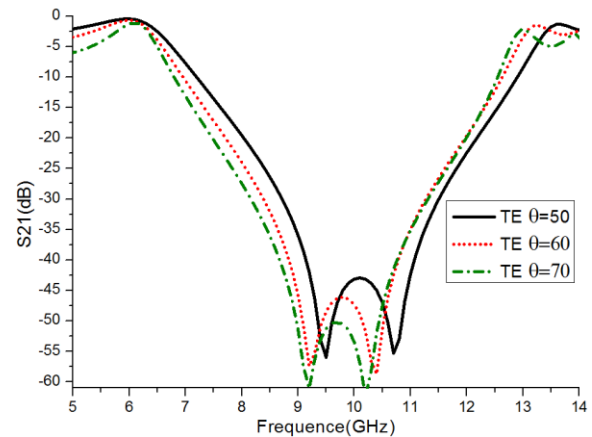
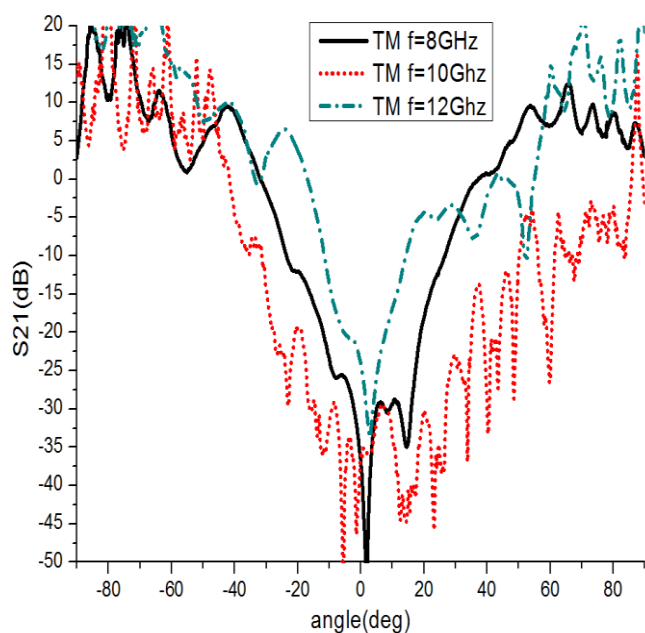


Fig. 2(a) shows one unit-cell of the two-dimensional periodic structure. For a vertical polarized incident wave, each horizontal gap between two square patches on the top surface acts as a capacitor, whose capacitance can be easily controlled by changing the width and length of the gap, namely, changing the size of the patch. In addition, the patch itself also provides an inductance with a small value connected in series with the capacitor. Part B of Fig. 2(b) gives the equivalent circuit of the periodic patches. At the bottom, the square apertures (or metal grids) can be envisioned as composed of long rods acting as inductors, whose inductance can be altered by changing the size of the aperture, while the horizontal bars will act primarily like capacitors in parallel with the inductors, as shown in Part

D of Fig. 2(b). Due to the large separation between the horizontal bars, the equivalent capacitance is also small. It is worth noting that neither the patches on the top nor the square apertures at the bottom can produce a resonance because of the small values of  $\epsilon_s$  and  $\mu_s$ . Consequently, the patches and the square apertures keep capacitive and inductive, respectively, over a wide frequency band for a normal incident wave.

The symmetry of the loop makes the stable performance at different azimuth angles available. The analysis of the proposed FSS structure is completed by using the Ansoft HFSS software. As shown in Figure 3 and Figure 4, a wide stop band can be obtained which is 5 GHz under -10 dB for TE mode wave and more than 2 GHz for TM mode. It can be seen that a relative bandwidth up to 50% and 20% for TE and TM mode waves have been achieved for incidence angle is  $60^\circ$ , respectively. For different pitch angles, TE wave exists a small frequency offset, and the bandwidth of TM wave becomes narrow as the pitch angle increases. In a large incident angle, the electrical length of cell is different for different polarization resulting bandwidth difference. Compared to the large angle of incidence, periodic structures characteristics are more clearly demonstrated for a small angle of incidence.



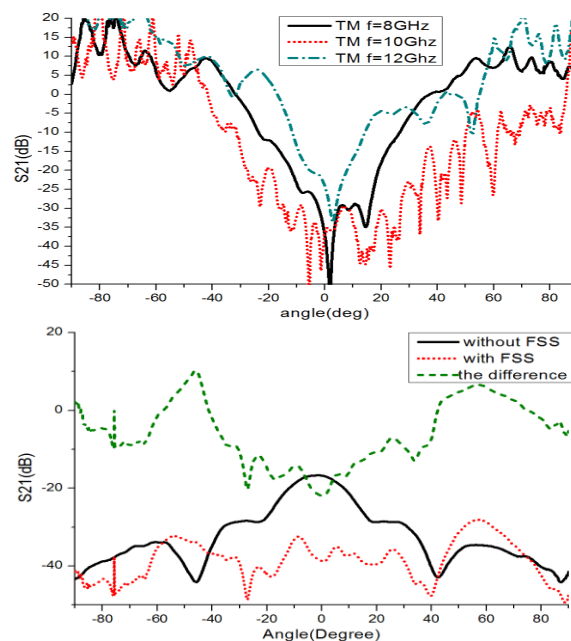


Another important characteristic of the antenna, the radiation pattern, has also been investigated. The co-polarization and cross-polarization in  $\phi$ -plane ( $\phi$ ) and  $\theta$ -plane ( $\theta$ ) at 9 GHz, 10 GHz and 11 GHz are plotted in Fig. 14. The peak radiation all happens in the broadside direction through the operating band. Measured side lobes are less than -12 dB and cross-polarizations are less than -12dB. Good agreements between simulated and measured main lobes are reached, while the side lobes of the measured patterns are higher than those of the simulated ones.

This discrepancy is probably attributed to the reflection and radiation from the cable and bracket used to feed and fix the antenna under test. Furthermore, electric fields with low levels are also more easily to be disturbed. Calculated cross-polarization patterns are lower than -35dB, so that we ignore them in the graphs. Due to the symmetric configuration of the EBG layer, the polarization of the antenna keeps consistent with that of the feeding antenna, which implies that this radiation characteristic can be easily altered by employing a feeding antenna with a different polarization. For instance, if a circularly polarized antenna is used as the feed, the radiation of the FP resonator antenna will also be circularly polarized.

## 5. CONCLUSION

A Fabry-Perot resonator antenna with a wide gain bandwidth in X band is presented. To extract the values of the lumped elements in the equivalent circuit is also discussed. Through the comparison between the results extracted from the equivalent circuit and those from the full-wave simulation, the model and analysis have been well validated.



## REFERENCES

- [1] S.-W. Qu and K. B. Ng, "Wideband millimeter-wave cavity-backed bowtie antenna," *Progr. Electromagn. Res.*, vol. 133, pp. 477–493, 2013.
- [2] P. Fei, Y. Qi, and Y.-C. Jiao, "Wide slot loop antenna with distance adjustable back-reflector for multiple narrowband antennas replacement," *Progr. Electromagn. Res.*, vol. 135, pp. 563–581, 2013.
- [3] C. Z. Hua, X. D. Wu, N. Yang, and W. Wu, "Millimeter-wave homogenous cylindrical lens antenna for multiple fan-beam scanning," *J. Electromagn. Waves Applicat.*, vol. 26, no. 14–15, 2012.
- [4] O. Xu, "Diagonal horn Gaussian efficiency enhancement by dielectric loading for submillimeter wave application at 150 GHz," *Progr. Electromagn. Res.*, vol. 114, pp. 177–194, 2011.
- [5] Sarabandi, K. and N. Behdad, *A frequency selective surface with miniaturized elements*. Antennas and Propagation, IEEE Transactions on, 2007. **55**(5): p. 1239-1245.
- [6] Meng, X. and A. Chen. *Influence of cross-loop slots FSS structure parameters on frequency response*. In *Microwave, Antenna, Propagation and EMC Technologies for Wireless Communications, 2009 3rd IEEE International Symposium on*. 2009. IEEE.
- [7] Munk, B.A., *Frequency selective surfaces: theory and design*. 2005: Wiley-Interscience. [8] L. Leger, C. Serier, R. Chantalat, M. Thevenot, T. Monediere, and B.
- [8] Jecko, "1-D dielectric EBG resonator antenna design," *Annal. Télécommun.*, vol. 59, no. 3–4, pp. 242–260, 2004.
- [9] B. A. Zeb, Y. Ge, K. P. Esselle, S. Zhu, and M. E. Tobar, "A simple dual-band electromagnetic band gap resonator antenna based on inverted reflection phase gradient," *IEEE Trans. Antennas Propag.*, vol. 60, no. 10, pp. 4522–4529, Oct. 2012.
- [10] Y. J. Lee, J. Yeo, R. Mittra, and S. P. Wee, "Application of electromagnetic bandgap (EBG) superstrates with controllable defects for a class of patch antennas as spatial angular filters," *IEEE Trans. Antennas Propag.*, vol. 53, no. 1, pp. 224–235, Jan. 2005.
- [11] A. R. Vaidya, R. K. Gupta, S. K. Mishra, and J. Mukherjee, "High-gain low side lobe level Fabry Perot cavity antenna with feed patch array," *Progr. Electromagn. Res.*, vol. 28, pp. 223–238, 2012.
- [12] J. R. Kelly, T. Kokkinos, and A. P. Feresidis, "Analysis and design of sub-wavelength resonant cavity type 2-D leaky-wave antennas," *IEEE Trans. Antennas Propag.*, vol. 56, no. 9, pp. 2817–2825, Sep. 2008.